Quantum Molecular Dynamics Simulations for the Nonmetal-to-Metal Transition in Fluid Helium

André Kietzmann, Bastian Holst, and Ronald Redmer
Universität Rostock, Institut für Physik, D-18051 Rostock, Germany

Michael P. Desjarlais and Thomas R. Mattsson
Pulsed Power Sciences Center, Sandia National Laboratories, Albuquerque, New Mexico 87185-1186, USA
(Received 16 January 2007; published 9 May 2007)

We have performed quantum molecular dynamics simulations for dense helium to study the nonmetal-to-metal transition at high pressures. We present new results for the equation of state and the Hugoniot curve in the warm dense matter region. The optical conductivity is calculated via the Kubo-Greenwood formula from which the dc conductivity is derived. The nonmetal-to-metal transition is identified at about 1 g/cm^3. We compare with experimental results as well as with other theoretical approaches, especially with predictions of chemical models.

DOI: 10.1103/PhysRevLett.98.190602 PACS numbers: 05.70.Ce, 52.25.Fi, 52.25.Kn, 52.65.Yy

The investigation of the phase diagram of hydrogen and helium, especially at extreme conditions of pressure and temperature, is not only of fundamental interest but also an indispensable prerequisite for astrophysics. For instance, thermophysical properties of hydrogen-helium mixtures determine the structure and evolution of stars, White Dwarfs, and Giant Planets [1–3]. The detection of Jupiter-like planets orbiting neighboring stars [4] has initiated a renewed interest in planetary physics. All planetary models require accurate equation-of-state data in order to solve the hydrostatic equation. While the limiting cases of low and high densities are well understood within chemical and plasma models, the intermediate region is much more complex. A nonmetal-to-metal transition occurs in hydrogen and helium at pressures of several megabar and temperatures of few eV, which implies a strong state dependence of the interparticle interactions and, thus, also of the thermodynamic variables. In this Letter, we study this *warm dense matter* region where the uncertainties in the equation-of-state data, both experimentally and theoretically, are greatest.

A lot of effort has been used to understand the behavior of warm dense hydrogen [5,6]. Although the simplest element in the periodic table, the transition of a nonconducting molecular liquid to an atomic or plasmalike conducting fluid at high pressure is still not fully understood [7–9]. Otherwise, helium is particularly suitable for the study of the high-pressure behavior since no dissociation equilibrium between molecules and atoms interferes with the ionization equilibrium, and the first (24.6 eV) and second ionization energy (54.4 eV) are well separated. Surprisingly, only few experimental and theoretical studies exist for warm dense helium [10–12].

In this Letter, we perform the first comprehensive *ab initio* study of the high-pressure behavior of helium. We determine the equation of state (EOS) in the warm dense matter region by means of quantum molecular dynamics (QMD) simulations. The Hugoniot curve is derived and compared with experimental points [13], other *ab initio* calculations [14], as well as with results of efficient chemical models [10–12]. Finally, we derive the electrical conductivity from the Kubo-Greenwood formula [15] and compare with shock-wave experimental data [16] in order to locate the nonmetal-to-metal transition.

QMD simulations are a powerful tool to calculate the structural, thermodynamic, and optical properties of warm dense matter in a combined first-principles approach. Details of this method have been described elsewhere [17–20]. We have performed QMD simulations employing a finite temperature Fermi occupation of the electronic states using Mermins approach (FT-DFT) [21] which is implemented in the plane wave density functional code VASP (Vienna *ab initio* simulation package) [22]. We consider 32 to 64 atoms in the simulation box and periodic boundary conditions. The electron wave functions are calculated using the projector augmented wave potentials [23] supplied with VASP [22], which yield more accurate conductivity results compared with other pseudopotentials. The exchange-correlation functional is calculated within the generalized gradient approximation (GGA) using the parameterization of Perdew, Burke, and Ernzerhof [24].

The convergence of the thermodynamic quantities in QMD simulations is an important issue [25]. We have chosen a plane wave cutoff E_{cut} at 700 eV so that the pressure is converged within 2% accuracy. We have also checked the convergence with respect to a systematic enlargement of the $\mathbf{k}$-point set in the representation of the Brillouin zone. Higher-order $\mathbf{k}$ points modify the EOS data only within 2% and the conductivity results up to a maximum of 10% relative to a one-point result. Therefore, we have restricted our calculations to the Γ point for the EOS and the mean value point $(1/4, 1/4, 1/4)$ for the conductivity.

The simulations were performed for a canonical ensemble where the temperature, the volume of the simulation box, and the particle number in the box are conserved quantities. The ion temperature is regulated by a Nosé-Hoover thermostat and the electronic temperature is fixed by Fermi weighting the occupation of bands [22]. After about hundred time steps the system is equilibrated and the subsequent 400 to 1000 time steps are taken to calculate the EOS data as running averages.

Results for the EOS of warm dense helium are given in Fig. 1. The isotherms of the pressure behave very systematically with temperature and density and show no indications of an instability such as the plasma phase transition at lower temperatures, contrary to results derived within the chemical picture [10–12]. For instance, the EOS of Winisdoerffer and Chabrier (WC) [12] is based on a free energy minimization schema for a mixture of helium atoms, single and double charged ions, and free electrons. Correlations are taken into account based on effective two-particle potentials. It agrees well with our QMD results for the pressure up to about 1 g/cm^3 and for ultrahigh densities above about 50 g/cm^3. However, this chemical model shows a systematic trend to lower pressures in the intermediate, strongly coupled region where the QMD results already approach an almost temperature-independent behavior as characteristic of a degenerate electron gas. These results underline the significance of *ab initio* calculations for warm dense matter states and will have a strong impact on calculations of planetary interiors [26]. Furthermore, we can identify the region where efficient chemical models are applicable in favor of time-consuming *ab initio* calculations.

Based on this EOS data, we have determined the Hugoniot curve via the condition

$$(E - E_0) = \tfrac{1}{2}(P + P_0)(V_0 - V), \qquad (1)$$

which relates all final states of a shock-wave experiment (E, P, V) with the initial state (E_0, P_0, V_0). We have used the values $E_0 = 20$ J/g, $T_0 = 4$ K, $P_0 = 1$ bar $\ll P$, and $V_0 = 32.4$ cm^3/mol ($\varrho_0 = 0.1235$ g/cm^3) for the first shock and $E_1 = 57$ kJ/g, $T_1 = 15\,000$ K, $P_1 = 190$ kbar, and $V_1 = 9.76$ cm^3/mol ($\varrho_1 = 0.41$ g/cm^3) for the second shock. We compare our results with double-shock experiments of Nellis *et al.* [13], with recent density-functional theory molecular dynamic simulation (DFT-MD) calculations of Militzer [14], and with two chemical models [12,27] in Fig. 2.

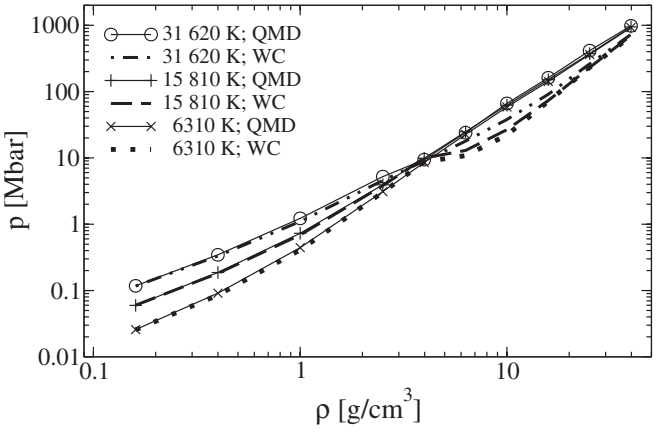

FIG. 1. Pressure isotherms in comparison with the WC free energy model [12].

A very good agreement is found with the double-shock experiments as well as with the other theoretical Hugoniot curves up to about 1 g/cm^3 which results from the accordance of the EOS data up to this density as mentioned above. A central problem in this context is the value and location of the maximum compression ratio $\eta_{\max}$. The chemical model FVT$^+_{\rm id}$ [27] is based on fluid variational theory and considers an ideal ionization equilibrium in addition. This model predicts a value of 5.5 at 375 GPa and 50 000 K if the second shock of the experiment is taken as initial state. Militzer [14] found a maximum compression of 5.24 at 360 GPa by using an EOS composed of DFT-MD without accounting for excited electronic states for lower temperatures (as shown in Fig. 2), FT-DFT post-processing of snapshots at intermediate temperature, and finally path integral Monte Carlo (PIMC) data in the high-temperature limit. Note that our QMD calculation yields the ionic motion based on the self-consistent thermal ground state of the system, which is not equivalent to postprocessing by applying a thermal occupation of electron states for snapshots obtained in a zero-Kelvin electronic structure calculation, as performed in [14]; for details see [28].

The QMD simulations were performed up to 1.5 g/cm^3, 350 GPa, and 60 000 K where the maximum compression ratio has not been reached yet. For still higher temperatures the number of bands increases drastically beyond the scope

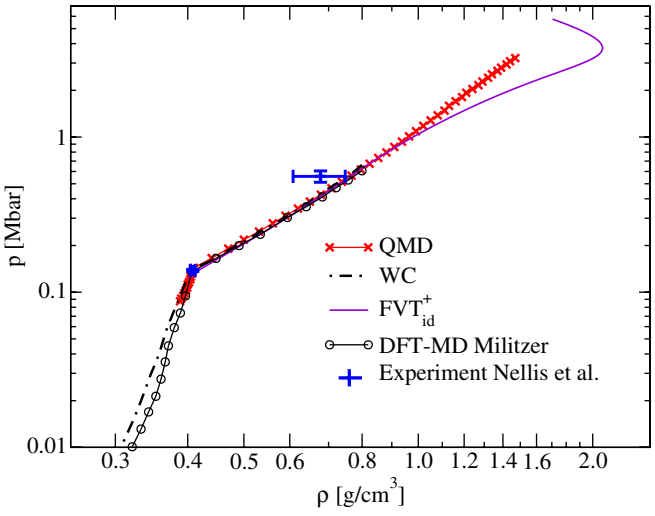

FIG. 2 (color online). Hugoniot curve for helium: QMD results are compared with double-shock experiments [13], DFT-MD results [14] without accounting for excited electronic states, and two chemical models WC [12] and FVT$^+_{\rm id}$ [27].

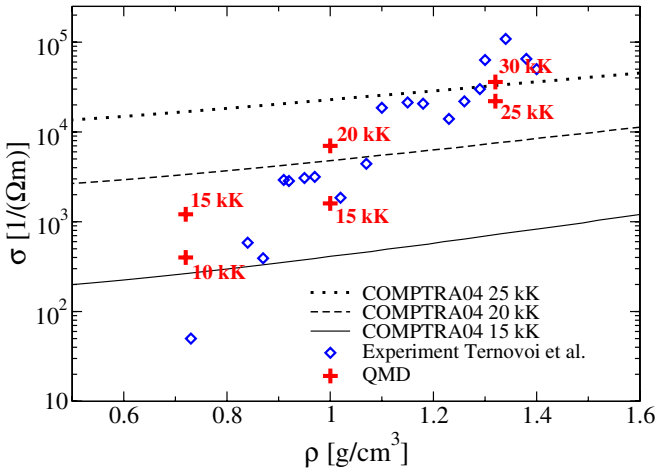

FIG. 3 (color online). QMD results for the static conductivity are compared with shock-wave experiments of Ternovoi *et al.* [16] between $(15-25)\times 10^3$ K and isotherms of the COMPTRA04 model [33]; temperatures are indicated.

of our computer capacity. Besides PIMC simulations [14], orbital-free DFT methods may be applicable in that high-temperature region [29]. Interestingly, the maximum compression ratio for helium ($\eta_{\max} \geq 5$) is greater than that for hydrogen ($\eta_{\max} = 4.25$); see, e.g., [6] for a more detailed discussion.

The dynamic conductivity $\sigma(\omega)$ is derived from the Kubo-Greenwood formula [15]

$$\sigma(\omega) = \frac{2\pi e^2\hbar^2}{3m^2\omega\Omega}\sum_{\mathbf{k}} W(\mathbf{k}) \sum_{j=1}^{N}\sum_{i=1}^{N}\sum_{\alpha=1}^{3}[F(\epsilon_{i,\mathbf{k}}) - F(\epsilon_{j,\mathbf{k}})] \times |\langle\Psi_{j,\mathbf{k}}|\nabla_\alpha|\Psi_{i,\mathbf{k}}\rangle|^2 \delta(\epsilon_{j,\mathbf{k}} - \epsilon_{i,\mathbf{k}} - \hbar\omega), \quad (2)$$

where e is the electron charge and m its mass. The summations over i and j run over N discrete bands considered in the electronic structure calculation for the cubic supercell volume Ω. The three spatial directions are averaged by the α sum. $F(\epsilon_{i,\mathbf{k}})$ describes the occupation of the ith band corresponding to the energy $\epsilon_{i,\mathbf{k}}$ and the wave function $\Psi_{i,\mathbf{k}}$ at $\mathbf{k}$. The δ-function has to be broadened because a discrete energy spectrum results from the finite simulation volume [17]. Integration over the Brillouin zone is performed by sampling special $\mathbf{k}$ points [30], where $W(\mathbf{k})$ is the respective weighting factor. Restricting the evaluations to the Baldereschi mean value point [31] yields converged results of better than 10% accuracy, see above.

The dc conductivity follows from Eq. (2) in the limit $\omega \to 0$. We compare with isentropic compression experiments of Ternovoi *et al.* [16] performed in the range $(15-25)\times 10^3$ K and predictions of the partially ionized plasma model COMPTRA04 [32,33] in Fig. 3. The experimental points show a very strong increase between 0.7 and 1.4 g/cm^3 indicating that a nonmetal-to-metal transition occurs. Adopting the Mott criterion for the minimum metallic conductivity also for finite temperatures, this transition can be located at about 20 000/Ωm and 1.3 g/cm^3.

TABLE I. Comparison of EOS data inferred from the experiment [16] and QMD data.

ρ [g/cm^3]	T [K]	p_{exp} [kbar]	p_{QMD} [kbar]
0.73	16 700	500	478
1.02	19 400	900	892
1.38	23 500	1685	1639

The QMD results reproduce the strong increase found experimentally very well except for the lowest density of 0.72 g/cm^3 where the experimental value is substantially lower than the QMD result.

The COMPTRA04 model [32,33] calculates the ionization degree and, simultaneously, the electrical conductivity accounting for all scattering processes of free electrons in a partially ionized plasma. This approach describes the general trends of the electrical conductivity with the density and temperature as found experimentally, see [34]. The isotherms displayed in Fig. 3 cover almost the range of the experimental points and agree also with the QMD data so that the nonmetal-to-metal transition is reproduced qualitatively well.

The strong influence of the temperature on the dc conductivity in this transition region can be seen by comparing the QMD results for two temperatures at the same density point; see Fig. 3. In order to exclude systematic errors from the experimental temperature determination, we have performed EOS calculations for the experimental points and compare typical values in Table I. A very good agreement is obtained so that the discrepancy in the conductivity data for the lowest density stems probably from the band gap problem of DFT. In order to solve this problem, DFT calculations beyond the GGA have to be performed by using, e.g., exact exchange formalisms [35] or quasiparticle calculations [36]. Although the computational requirements of such extended electronic structure calculations in QMD is well beyond the capacity of present resources, their implementation will be an important subject of future work in this area.

The origin of this nonmetal-to-metal transition can be elucidated by inspecting the variation of the density of

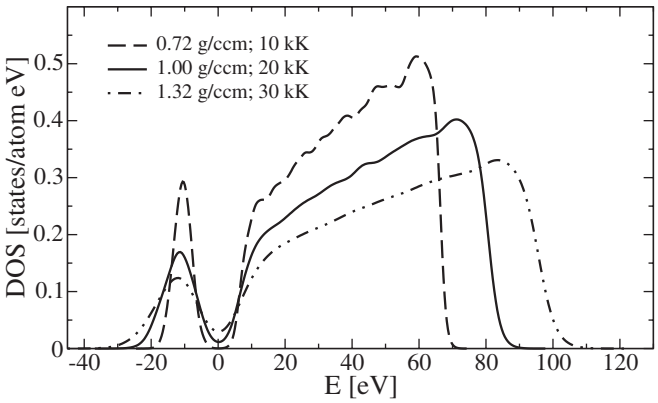

FIG. 4. DOS as function of the energy for three typical situations. The Fermi energy is located at zero.

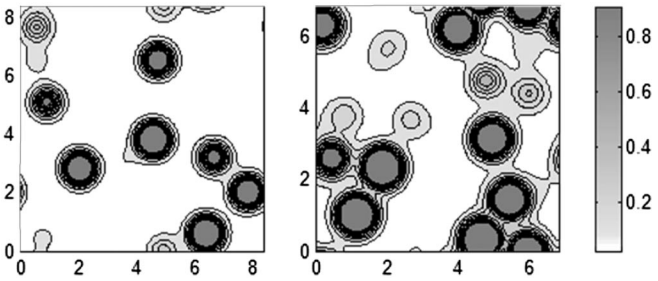

FIG. 5. Typical contour plot of the charge density in units of $e/\text{Å}^3$ for 0.72 g/cm^3 at 10 000 K (left) and 1.32 g/cm^3 at 30 000 K (right) along a slice through the simulation box; x and $y$axis are also given in units of Å.

states (DOS) along the path of the shock-wave experiments, see Fig. 4. For the lowest density of 0.72 g/cm^3, a gap still exists in the DOS so that thermally activated electron transport occurs as in semiconductors. With increasing density, the gap region is slightly reduced. The main effect is, however, that electronic states fill up the region of the Fermi energy with increasing temperature so that a higher, metal-like conductivity follows; see also [8].

This behavior is also revealed from the change of the charge density with increasing mass density as shown in Fig. 5. The electrons are still localized for the lower density representing an atomic fluid (left panel), while transient filaments and clusters occur for the higher density which indicates a metal-like behavior (right panel). A similar behavior has been found for the expanded fluid alkali metals Rb and Cs [37].

In summary, we have determined the thermophysical properties of dense helium within an *ab initio* approach. The results show clearly the strong influence of quantum effects and correlations in the warm dense matter region. The nonmetal-to-metal transition occurs at about 1 g/cm^3, in good agreement with shock-wave experimental data. These new results will have a strong influence on models for planetary interiors.

We thank P. M. Celliers, V. E. Fortov, B. Militzer, V. B. Mintsev, G. Röpke, and V. Ya. Ternovoi for stimulating discussions and for providing us with their data. This work was supported by the Deutsche Forschungsgemeinschaft within the SFB 652 and the Grant No. mvp00006 of the supercomputing center HLRN. Sandia is a multiprogram laboratory operated by Sandia Corporation, a Lockheed Martin Company, for the United States Department of Energy's National Nuclear Security Administration under Contract No. DE-AC04-94AL85000.

[1] D. Saumon, G. Chabrier, and H. M. Van Horn, Astrophys. J. Suppl. Ser. **99**, 713 (1995).
[2] V. Ya. Ternovoi *et al.*, JETP Lett. **79**, 6 (2004).
[3] J. Vorberger, I. Tamblyn, B. Militzer, and S. A. Bonev, Phys. Rev. B **75**, 024206 (2007).
[4] M. A. C. Perryman, Rep. Prog. Phys. **63**, 1209 (2000); See also http://exoplanet.eu for up to date information.
[5] Special issue on Hydrogen at High Pressure edited by D. A. Young and R. Cauble [High Pressure Research **16**,281 (2000)].
[6] W. J. Nellis, Rep. Prog. Phys. **69**, 1479 (2006).
[7] N. W. Ashcroft, Phys. Rev. B **41**, 10963 (1990); K. Johnson and N. W. Ashcroft, J. Phys. Condens. Matter **10**, 11 135 (1998).
[8] L. A. Collins *et al.*, Phys. Rev. B **63**, 184110 (2001).
[9] R. Redmer, G. Röpke, S. Kuhlbrodt, and H. Reinholz, Phys. Rev. B **63**, 233104 (2001).
[10] A. Förster, T. Kahlbaum, and W. Ebeling, Laser Part. Beams **10**, 253 (1992); T. Kahlbaum and A. Förster, Fluid Phase Equilib. **76**, 71 (1992).
[11] M. Schlanges, M. Bonitz, and A. Tschttschjan, Contrib. Plasma Phys. **35**, 109 (1995).
[12] C. Winisdoerffer and G. Chabrier, Phys. Rev. E **71**, 026402 (2005).
[13] W. J. Nellis *et al.*, Phys. Rev. Lett. **53**, 1248 (1984).
[14] B. Militzer, Phys. Rev. Lett. **97**, 175501 (2006).
[15] R. Kubo, J. Phys. Soc. Jpn. **12**, 570 (1957); D. A. Greenwood, Proc. Phys. Soc. London **71**, 585 (1958).
[16] V. Ya. Ternovoi *et al.*, AIP Conf. Proc. **620**, 107 (2002).
[17] M. P. Desjarlais, J. D. Kress, and L. A. Collins, Phys. Rev. E **66**, 025401 (2002).
[18] M. P. Desjarlais, Phys. Rev. B **68**, 064204 (2003).
[19] Y. Laudernet, J. Clérouin, and S. Mazevet, Phys. Rev. B **70**, 165108 (2004).
[20] J. Clérouin *et al.*, Phys. Rev. B **71**, 064203 (2005).
[21] N. D. Mermin, Phys. Rev. **137**, A1441 (1965).
[22] G. Kresse and J. Hafner, Phys. Rev. B **47**, 558 (1993); **49**, 14 251 (1994); G. Kresse and J. Furthmüller, Phys. Rev. B **54**, 11 169 (1996).
[23] P. E. Blöchl, Phys. Rev. B **50**, 17 953 (1994); G. Kresse and D. Joubert, Phys. Rev. B **59**, 1758 (1999).
[24] J. P. Perdew, K. Burke, and M. Ernzerhof, Phys. Rev. Lett. **77**, 3865 (1996).
[25] A. E. Mattsson *et al.*, Model. Simul. Mater. Sci. Eng. **13**, R1 (2005).
[26] D. Saumon and T. Guillot, Astrophys. J. **609**, 1170 (2004).
[27] V. Schwarz, H. Juranek, and R. Redmer, Phys. Chem. Chem. Phys. **7**, 1990 (2005).
[28] T. R. Mattsson and M. P. Desjarlais, Phys. Rev. Lett. **97**, 017801 (2006).
[29] F. Lambert, J. Clérouin, and G. Zerah, Phys. Rev. E **73**, 016403 (2006).
[30] H. J. Monkhorst and J. D. Pack, Phys. Rev. B **13**, 5188 (1976).
[31] A. Baldereschi, Phys. Rev. B **7**, 5212 (1973).
[32] S. Kuhlbrodt, B. Holst, and R. Redmer, Contrib. Plasma Phys. **45**, 73 (2005).
[33] S. Kuhlbrodt *et al.*, Contrib. Plasma Phys. **45**, 61 (2005).
[34] V. E. Fortov *et al.*, J. Exp. Theor. Phys. **97**, 259 (2003).
[35] R. P. Muller and M. P. Desjarlais, J. Chem. Phys. **125**, 054101 (2006).
[36] P. Rinke *et al.*, New J. Phys. **7**, 126 (2005); S. V. Faleev *et al.*, Phys. Rev. B **74**, 033101 (2006).
[37] A. Kietzmann *et al.*, J. Phys. Condens. Matter **18**, 5597 (2006).